NIH Public Access
Author Manuscript
Cell Stem Cell. Author manuscript; available in PMC 2011 August 6.

Published in final edited form as:
Cell Stem Cell. 2010 August 6; 7(2): 174–185. doi:10.1016/j.stem.2010.06.014.

Hematopoietic stem cell quiescence promotes error prone DNA repair and mutagenesis

Mary Mohrin[1], **Emer Bourke**[2], **David Alexander**[3], **Matthew R. Warr**[1], **Keegan Barry-Holson**[1], **Michelle M. Le Beau**[4], **Ciaran G. Morrison**[2], and **Emmanuelle Passegué**[1,*]

[1] The Eli and Edythe Broad Center for Regenerative Medicine and Stem Cell Research, Department of Medicine, Division of Hematology/Oncology, University of California San Francisco, San Francisco, California, 94143, USA [2] Centre for Chromosome Biology, School of Natural Sciences, National University of Ireland Galway, Galway, Ireland [3] University of California Santa Cruz, Santa Cruz, California, 95064, USA [4] University of Chicago, Section of Hematology/Oncology and the Comprehensive Cancer Center, Chicago, Illinois, 60637, USA

SUMMARY

Most adult stem cells, including hematopoietic stem cells (HSCs), are maintained in a quiescent or resting state *in vivo*. Quiescence is widely considered to be an essential protective mechanism for stem cells that minimizes endogenous stress caused by cellular respiration and DNA replication. Here, we demonstrate that HSC quiescence can also have detrimental effects. We found that HSCs have unique cell-intrinsic mechanisms ensuring their survival in response to ionizing irradiation (IR), which include enhanced pro-survival gene expression and strong activation of p53-mediated DNA damage response. We show that quiescent and proliferating HSCs are equally radioprotected but use different types of DNA repair mechanisms. We describe how nonhomologous end joining (NHEJ)-mediated DNA repair in quiescent HSCs is associated with acquisition of genomic rearrangements, which can persist *in vivo* and contribute to hematopoietic abnormalities. Our results demonstrate that quiescence is a double-edged sword that renders HSCs intrinsically vulnerable to mutagenesis following DNA damage.

INTRODUCTION

DNA repair is essential for cell survival and maintenance of tissue homeostasis (Lombard et al., 2005). Cellular organisms must constantly contend with endogenous DNA damage caused by intrinsic or extrinsic stresses and have evolved multiple DNA repair systems to deal with these insults (Sancar et al. 2004). DNA double-strand breaks (DSB) are considered the most cytotoxic type of DNA lesion and can arise during DNA replication or upon exposure to ionizing radiation (IR) and radiomimetic chemicals. DSB formation triggers a global DNA damage response resulting in the activation of the DNA damage sensor ATM, which in turn activates cell cycle checkpoints and phosphorylates an array of downstream targets including the tumor suppressor gene p53. This global DNA damage response (DDR) is directed toward the cells' own preservation and can lead to growth arrest and initiation of

[*]Corresponding author: Emmanuelle Passegué, PhD, University of California San Francisco, 513 Parnassus Avenue, MSB-1471E, Box 0525 San Francisco, CA 94143-0525, USA, Phone: 415-476-2426, Fax: 415-514-2346 passeguee@stemcell.ucsf.edu.

Publisher's Disclaimer: This is a PDF file of an unedited manuscript that has been accepted for publication. As a service to our customers we are providing this early version of the manuscript. The manuscript will undergo copyediting, typesetting, and review of the resulting proof before it is published in its final citable form. Please note that during the production process errors may be discovered which could affect the content, and all legal disclaimers that apply to the journal pertain.

NIH-PA Author Manuscript
NIH-PA Author Manuscript
NIH-PA Author Manuscript

NIH-PA Author Manuscript

NIH-PA Author Manuscript

NIH-PA Author Manuscript

DNA repair by specialized DSB repair mechanisms, with programmed cell death being an alternative outcome of excessive or unrepaired DNA damage. The two principal and complementary mechanisms by which eukaryotic cells repair DSBs are homologous recombination (HR) and nonhomologous end joining (NHEJ) (Sancar et al., 2004). HR-mediated DNA repair uses a template for accurate repair, usually the sister chromatid, and thus can only occur in cycling cells. In contrast, NHEJ-mediated DNA repair has a limited requirement for sequence homology and can take place at any stage of the cell cycle. NHEJ-type repair is a more error-prone mechanism than the high fidelity HR-type repair, which often leads to misrepaired DSBs that may result in chromosomal deletions, insertions or translocations and subsequent genomic instability (Weinstok et al., 2006). While defects in DNA damage responses have been associated with cancer, aging and stem cell abnormalities (Hanahan and Weinberg, 2000; Park and Gerson, 2005), much remains to be learned about the mechanism by which stem cells normally respond to DNA damage and repair DSBs.

The hematopoietic system provides a uniquely tractable model to investigate the activity of specific cell populations (Orkin and Zon, 2008). Hematopoietic development is organized hierarchically, starting with a rare population of hematopoietic stem cells (HSCs) that gives rise to a series of committed progenitors and mature cells with exclusive functional and immunophenotypic properties. HSCs are the only cells within the hematopoietic system that self-renew for life, whereas other hematopoietic progenitors cells are short-lived and committed to the transient production of mature blood cells. Under steady-state conditions, HSCs are a largely quiescent, slowly cycling cell population, which, in response to environmental cues, are capable of dramatic expansion and contraction to ensure proper homeostatic replacement of blood cells. In this context, the quiescent status of HSCs is widely considered to be an essential protective mechanism that minimizes endogenous stress caused by cellular respiration and DNA replication (Orford and Scadden, 2008). Proper execution of DNA repair processes is essential for normal HSC functions. Mice lacking components and regulators of the DNA damage response and DSB repair mechanisms all display severe hematopoietic phenotypes and HSC defects (Ito et al., 2004; Nijnik et al., 2007; Rossi et al., 2007). Defective DNA repair has also been associated with a spectrum of human blood disorders (Wang, 2007) and the occurrence of chromosomal translocations is a hallmark of human hematological malignancies (Look et al., 1997). Previous studies have shown that genotoxic insults such as ionizing radiation (IR) differentially affect subsets of bone marrow hematopoietic cells, with HSCs being more radioresistant than their downstream myeloid progeny (Meijne et al., 1991; Down et al., 1995). This result is consistent with the low levels of intracellular oxidative species (ROS) observed in HSCs compared to myeloid progenitors (Tothova et al., 2007) and the well-established link between irradiation-induced DNA damage and ROS generation. However, limited information is currently available about the precise DNA repair capacity of HSCs and myeloid progenitor cells as well as on the mutagenic consequences of such repair for their biological functions.

Here, we use flow cytometry to isolate a highly enriched HSC-containing population referred to as hematopoietic stem and progenitor cells (HSPCs) and two distinct subsets of myeloid progenitors (MPs), the common myeloid progenitors (CMPs) and the granulocyte/macrophage progenitors (GMPs). We show that long-lived HSPCs have robust and unique cell-intrinsic mechanisms to ensure their survival in response to IR exposure, which include enhanced pro-survival gene expression and a strong induction of p53-mediated DDR leading to growth arrest and DNA repair; whereas short-lived MPs are molecularly poised to undergo apoptosis and are predominantly eliminated in response to genotoxic stress. Most importantly, we demonstrate that HSPCs are forced to initiate DNA repair using the error-prone NHEJ mechanism due to their largely quiescent cell cycle status and the molecular composition of their DNA repair machinery. We show that this preferential use of NHEJ-

NIH-PA Author Manuscript

NIH-PA Author Manuscript

NIH-PA Author Manuscript

mediated DNA repair renders quiescent HSPCs susceptible to genomic instability associated with misrepaired DNA, which can contribute to HSC loss of function and/or pre-malignant transformation *in vivo*. In contrast, HSPCs that have been induced to proliferate, either by *in vitro* culturing or *in vivo* mobilization treatment, undergo DNA repair using the high fidelity HR mechanism and have a significantly decreased risk of acquiring mutation(s). Taken together, our results demonstrate that HSC quiescence is a double-edged sword, which on the one hand protects HSCs against endogenous stress but, on the other hand, renders HSCs intrinsically vulnerable to mutagenesis following DNA damage.

RESULTS

Enhanced radioresistance in HSPCs compared to MPs

We first defined the radiosensitivity of our purified hematopoietic stem and myeloid progenitor cells. We isolated HSPCs (Lin^-/c-Kit^+/Sca-1^+/$Flk2^-$), CMPs (Lin^-/c-Kit^+/Sca-1^-/$CD34^+$/$Fc\gamma R^-$) and GMPs (Lin^-/c-Kit^+/Sca-1^-/$CD34^+$/$Fc\gamma R^+$) from the pooled bone marrow of 5 to 10 wild type mice, exposed them to increasing doses of IR (0-10Gy) and performed clonogenic survival assays in methylcellulose and liquid media (Figures 1A and S1). We observed a striking difference in colony numbers at the 2Gy dose of irradiation, with HSPCs displaying significantly enhanced radioresistance compared to MPs that correlated with the differentiation status of the populations analyzed (HSPCs > CMPs > GMPs). At doses greater than 4Gy, all three populations were equally radiosensitive and did not form colonies, in agreement with the fact that the hematopoietic system is one of the first organ systems to fail after total body irradiation. To determine whether the enhanced radioresistance of HSPCs results from cell intrinsic differences in their DNA damage response, we performed a similar clonogenic survival assay with HSPCs and MPs isolated from *Atm*-deficient mice (Ito et al., 2004) (Figure 1B). In contrast to wild type cells, we found that $Atm^{-/-}$ HSPCs, CMPs and GMPs all displayed matching hypersensitivity to increasing doses of IR (0-4Gy). These results confirm that HSPCs are intrinsically more resistant to IR exposure than CMPs and GMPs, and indicate that ATM is an essential mediator of this differential DNA damage response. We also showed that Slam-HSCs (Lin^-/c-Kit^+/Sca-1^+/$Flk2^-$/$CD150^+$/$CD48^-$), one of the most pure HSC populations characterized so far, display radioresistance similar to that of HSPCs (Figure S1), which indicate that our analysis of HSPCs may be generalized in this instance to HSC biology.

HSPCs undergo growth arrest while MPs die in response to IR treatment

We then investigated the cellular outcomes (*i.e.*, proliferation and apoptosis responses) induced by 2Gy IR in HSPCs and MPs. CFSE dilution assays uncovered a profound delay in the division rates of 2Gy-irradiated HSPCs that was still evident 3 days after IR exposure (Figure 1C). While CMPs displayed an intermediate behavior, with a recovery of normal proliferation by 3–4 days post-IR, the irradiation treatment had almost no effect on GMP proliferation rates. We then measured the apoptotic response occurring in these cells using intracellular cleaved caspase 3 (CC3) and Annexin V/7-AAD staining (Figure 1D and data not shown). We found that unirradiated MPs had significantly higher basal levels of CC3 staining compared to HSPCs after 1 and 2 days in culture (~1.3 and 8.5-fold higher in CMPs and ~ 3.7- and 10.4-fold higher in GMPs, respectively). Furthermore, we observed a robust and immediate IR-mediated apoptotic response in CMPs and GMPs but a minimal induction of apoptosis 2 days after irradiation in HSPCs. To establish the status of the apoptotic machinery in these cells, we performed qRT-PCR analysis of the expression levels of a comprehensive panel of *bcl2* family pro- and anti-apoptotic genes in freshly isolated HSPCs, CMPs and GMPs (Figure 1E). We observed an overall deficit in pro-survival genes and a trend towards increased expression of pro-apoptotic genes in MPs compared to HSPCs. Using western blotting, we confirmed several highly significant changes ($p \leq 0.001$) found

NIH-PA Author Manuscript

NIH-PA Author Manuscript

NIH-PA Author Manuscript

at the mRNA level including decreased Mcl-1 and increased Bid proteins in GMPs (Figure 1F). To functionally test whether a deficit in pro-survival genes contributes to the higher rate of apoptosis in MPs, we isolated cells from H2k-*bcl2* transgenic mice (Domen et al., 2000) and evaluated the effect of enhanced *bcl2* expression on their apoptotic response (Figure 1D). While HSPCs remained essentially unaffected by *bcl2* overexpression, we observed a significant decrease in the basal level of CC3 staining in MPs, especially in GMPs. However, H2k-*bcl2* MPs displayed an unchanged IR-mediated apoptotic response, which suggests that overexpressing a single pro-survival gene cannot compensate for the strength of IR-mediated death signals in MPs. Taken together, these results suggest that the short-lived, expendable MPs (especially GMPs) are poised at the molecular level to undergo apoptosis due to a deficit in pro-survival genes and are mostly eliminated in response to IR treatment. In contrast, the long-lived HSPCs predominantly survive and undergo growth arrest following irradiation.

Dual role of the p53 pathway

p53 is an important downstream target of ATM, which can mediate either growth arrest or apoptosis following DNA damage. To determine whether HSPCs and MPs engage a p53-dependent DDR, we first treated mice with 2Gy IR and measured the changes in p53 protein levels occurring in these bone marrow compartments at 12 hours post-irradiation using intracellular FACS analysis (Figure 2A). While we observed stabilization of p53 protein in *in vivo* irradiated HSPCs, no significant changes were found in irradiated MPs. We also confirmed by immunoblot a ~2-fold stronger phosphorylation of p53 (Ser15) in HSPCs compare to MPs at 1 hour post-IR and a tailing off in both populations by 4 hours post-IR (Figure S2). To directly assess p53 activity in these compartments, we then measured the induction of p53 target genes (i.e, *bax*, *bak*, *noxa*, *p21*) by qRT-PCR using purified cells grown in liquid culture for 8 and 12 hours post-IR (Figure 2B). Interestingly, the strength of the p53-mediated DDR (as measured by the levels of target gene induction) was much higher and sustained for a longer time in HSPCs compared to the limited and transient response observed in MPs, especially in GMPs. We further confirmed the functional importance of p53 in both HSPCs and MPs using cells isolated from *Trp53*$^{-/-}$ mice (Liu et al., 2009). Analysis of *Trp53*$^{-/-}$ HSPCs, CMPs and GMPs both in clonogenic survival assays and liquid culture (Figure 2C and data not shown) revealed increased radioresistance in all three populations. Furthermore, we showed that removal of p53 prevents HSPCs from undergoing growth arrest following IR exposure (Figure 2D), while in MPs, p53 deletion considerably decreased the basal level and abrogated IR-mediated induction of apoptosis (Figure 2E). As expected, p53-mediated induction of *p21* and *bcl2* pro-apoptotic targets did not occur in irradiated *Trp53*$^{-/-}$ HSPCs and MPs (Figure 2F). Taken together, these results highlight the dual role that p53 plays in modulating opposite outcomes in irradiated HSPCs and MPs. We postulate that in HSPCs the high basal level of pro-survival genes coupled with the strong p53-mediated induction of *p21* protect against the killing effects of increased pro-apoptotic gene expression, resulting mainly in growth arrest as already observed in other cellular contexts (Abbas et al., 2009). In contrast, in MPs, the limited induction of pro-apoptotic genes that occurs in the context of very low basal levels of pro-survival genes and in the absence of or with weak induction of *p21*, results predominantly in cell death.

Ongoing DNA repair in HSPCs

To determine the extent of DSB DNA repair in irradiated HSPCs and MPs, we first used immunofluorescence microscopy to quantify γH2AX-containing ionizing radiation-induced foci (IRIF), which form at the sites of DNA damage (Figure 3A). Unirradiated HSPCs and MPs all displayed extremely low levels of IRIF and, following exposure to 2Gy IR, showed an immediate induction of γH2AX-positive DNA damage foci. By 4 hours to 24 hours post-IR, the numbers of IRIF declined in HSPCs with relatively faster kinetics than in MPs. To

NIH-PA Author Manuscript

NIH-PA Author Manuscript

NIH-PA Author Manuscript

determine whether the loss of γH2AX foci corresponded to ongoing DNA repair or simply reflected cell elimination, we next subjected unirradiated and irradiated cells to an alkaline COMET assay and scored the tail DNA content on a 0 (undamaged) to 4 (very damaged) scale to assess the severity of the resulting DNA damage (Figure 3B). We started this assay with identical numbers of cells for all conditions and normalized the tail DNA content score for the numbers of cells actually detected on the agarose slides, to account for the observation that dying cells are often lost during the various steps of this experimental procedure. Quantification of the results revealed that all three populations acquired equivalent amounts of DNA damage 2 hours after irradiation (Figure 3C and Table S1). By 24 hours post-IR, we observed a significant shift towards less damaged tail DNA content scores in HSPCs, which occurred without overall loss of cells thereby demonstrating active ongoing DNA repair. In contrast, in MPs, we predominantly observed cell elimination, with the persistence of only undamaged cells or a few cells undergoing DNA repair. Taken together, these results demonstrate that irradiated HSPCs survive and undergo DNA repair, and confirm that the majority of irradiated MPs are eliminated. They also highlight the fact that the decrease in γH2AX staining can be skewed due to the confounding impact of cell death (as in MPs) and, while marking the resolution of DSBs (as in HSPCs), cannot simply be equated with complete DNA repair.

Preferential use of NHEJ repair mechanism in quiescent HSPCs

We then investigated the type of DSB repair mechanisms used by irradiated HSPCs and the few surviving MPs. To assess HR activity, we quantified IRIF containing the Rad51 recombinase protein by immunofluorescence microscopy. Unfortunately, none of the components of the NHEJ machinery that we examined (Ku70, Ku80) were detectable by microscopy in IRIF (data not shown). Therefore, as a surrogate, we quantified IRIF containing the 53BP1 DNA damage response protein as 53BP1 has been shown to function, albeit not exclusively, in NHEJ. Rad51 IRIF formation occurred rapidly in irradiated MPs, reaching its maximum (~50% of the cells) by 2 hours (CMPs) and 4 hours (GMPs) post-IR and then remaining unchanged for up to 24 hours (Figure 4A). In contrast, no significant Rad51 recruitment was observed in HSPCs until 24 hours post-IR. This staining pattern is consistent with the proliferation index of the respective populations (Figures S3), with irradiated HSPCs being mostly quiescent at the start of the culture and only initiating their first cell division by ~ 24 hours *in vitro* (Figure 1C). Conversely, recruitment of 53BP1 in IRIF occurred immediately in all three populations but then declined at a slower rate in HSPCs (Figure 4B). To support these observations, we also analyzed the basal expression level of HR and NHEJ components in freshly isolated HSPCs, CMPs and GMPs (Figure 4C). Strikingly, we found that all of the HR components and/or regulators we investigated were expressed at significantly higher levels in MPs compared to HSPCs, while the NHEJ machinery components were either dramatically decreased (*Ku80*) or unchanged in MPs. Finally, we used a reporter assay in which the religation of a digested plasmid expressing the enhanced green fluorescent protein (eGFP) allowed a measurement of the NHEJ activity present at baseline and following IR in transfected cells (Figure S4). Consistent with the predominance of NHEJ as a repair mechanism in HSPCs, we observed high basal levels of NHEJ activity in unirradiated HSPCs and a ~2-fold increase following irradiation (Figures 4D and S4). In sharp contrast, GMPs displayed extremely low basal levels and no IR-mediated induction of NHEJ activity, whereas CMPs showed intermediary levels of basal and IR-mediated NHEJ activity. Taken together, these results demonstrate that HSPCs are forced to initiate DNA repair using NHEJ-type mechanisms due to their largely quiescent cell cycle status and the molecular wiring of their DNA repair machinery. They also indicate that the few proliferating MPs that escape IR-mediated cell killing are molecularly primed to undergo HR-mediated DNA repair and do not use NHEJ-type mechanisms.

NIH-PA Author Manuscript

NIH-PA Author Manuscript

NIH-PA Author Manuscript

HSPC radioprotection is independent of quiescence

It has been suggested that quiescence provides HSCs with enhanced resistance to genotoxic stress (Tothova et al., 2007; Orford and Scadden, 2008). To experimentally test this assumption, we forced HSPCs to proliferate before exposing them to 2Gy IR (Figure 5A). First, we pre-cultured resting HSPCs (Rest. HSPCs) for ~ 24 hours *in vitro* (24hr preC HSPCs) to induce their proliferation and, second, we used an *in vivo* mobilization treatment (Passegué et al., 2005) to harvest proliferating bone marrow HSPCs (Mob. HSPCs) after one injection of cyclophosphamide and two days of stimulation with G-CSF. Both strategies resulted in a net increase in HSPC cycling rates as measured after a 1-hour BrdU pulse (Figures 5B) and a loss of quiescence as measured by intracellular 7AAD/PyroninY staining (Figures 5C). Strikingly, no differences were observed in the radioresistance of proliferating HSPCs compared to resting HSPCs using either clonogenic survival assay in methylcellulose (Figure 5D) or proliferation in liquid culture (Figure 5E). At the molecular level, we found that proliferating HSPCs had decreased basal levels of pro-survival genes, varied levels of pro-apoptotic genes and constitutively higher apoptosis rates than quiescent HSPCs (Figures S5 and 5F). However, like quiescent HSPCs, proliferating HSPCs did not show a significant IR-mediated apoptotic response (Figure 5F), but unlike quiescent HSPCs, they did not undergo IR-mediated growth arrest and displayed an attenuated p53-mediated response including limited induction of *p21* expression (Figures 5G and S5). Altogether, these results indicate a major re-wiring of the DNA damage response in proliferating HSPCs to one that closely resembles the response observed in MPs. However, this does not result in an analogous loss of radioresistance suggesting that proliferative HSPCs still retain additional, yet unexplored, protective mechanism(s) that are not shared by their more differentiated progeny.

Access to HR repair in proliferating HSPCs

Next, we investigated the type of DNA repair mechanisms that were used by 2Gy-irradiated proliferating HSPCs. We observed similar kinetics of γH2AX IRIF induction and resolution in both resting and proliferating HSPCs, indicating that they are equally efficient at repairing IR-induced DSBs (Figure S5). However, in contrast to quiescent HSPCs, proliferating HSPCs immediately formed Rad51 IRIF, which reached maximum levels by 2–4 hours post-IR and remained elevated throughout the 24-hour experiment (Figure 6A). 53BP1 recruitment to IRIF also occurred immediately in proliferating HSPCs but sharply declined thereafter and returned to basal levels by 12 hours post-IR, in contrast to the slow decline seen in resting HSPCs (Figure 6B). Consistent with the rewiring of the DNA damage response, we also found increased expression of HR genes and decreased expression of NHEJ components in proliferating HSPCs compared to quiescent HSPCs (Figure 6C). While the basal levels of NHEJ activity were not significantly different in unirradiated cells (Figure S4), we observed a complete abrogation of IR-mediated induction of NHEJ activity in proliferating HSPCs compared to resting HSPCs (Figure 6D). Taken together, these results demonstrate that quiescence dramatically restricts HSPC ability to use the high-fidelity HR-mediated repair and instead forces them to rely on the more error-prone NHEJ mechanism to repair DSBs.

Quiescent HSPCs are prone to acquire mutations

NHEJ-mediated repair can be mutagenic in many ways, most commonly by causing deletion of microhomology sequences flanking the breakpoint or insertions at the DSB joint region. Since IR can induce DSBs anywhere in the genome, we used fluorescence *in situ* hybridization (FISH) in an attempt to determine whether NHEJ-mediated mutagenic repair could result in molecular-level deletions within a fragile chromosomal region, leading to loss of hybridization signals. Un-irradiated and 2Gy irradiated quiescent HSPCs were grown in culture for 4 to 5 days for maximal expansion, treated for 4 hours with Colcemid^{TM}, fixed

NIH-PA Author Manuscript

NIH-PA Author Manuscript

NIH-PA Author Manuscript

for cytogenetic studies and interphase cells were then hybridized with a probe for the mouse *Fhit* locus common fragile site. No significant difference in signal intensity could be observed between unirradiated and irradiated cells using this approach (Figure S6). More sensitive techniques will therefore be required to assess these particular forms of mutagenic NHEJ-mediated DSBs repair. NHEJ has also been shown to be very proficient at mediating chromosomal translocations, whereas HR-type repair are not because of crossover suppression (Weinstok et al., 2006). To determine whether the progeny of IR-treated resting HSPCs could acquire major genomic rearrangements as the result of inaccurate NHEJ-mediated DNA repair, and whether the frequency of such mutagenic events would be decreased in HR-competent, proliferating HSPCs, we performed spectral karyotyping (SKY) analysis on the metaphase cells obtained from the same cell preparations (Figure 7A). Strikingly, we found that more than 30% of the cells derived from IR-treated resting HSPCs consistently displayed major genomic rearrangements, including reciprocal translocations, interstitial deletions and complex rearrangements, compared to unirradiated cells (Figure 7B and Table S2). Most importantly, we showed that induction of proliferation and the availability of HR-mediated DNA repair in both 24h preC. and Mob. HSPCs significantly reduced the number and frequency of genomic aberrations occurring upon IR exposure, hence decreasing by half the risk of acquiring genomic instability in the self-renewing HSPC compartment (Figure 7C and Table S2). Taken together, these results provide a direct demonstration that IR-damaged HSPCs, which are limited to using NHEJ-repair mechanism by their quiescent status, are prone to acquire cytogenetic aberrations as a result of incorrectly repaired DNA damage.

Persistence of misrepaired HSPCs *in vivo*

We then tested whether such misrepaired HSPCs could persist *in vivo* and eventually contribute to hematological disorders. We transplanted unirradiated or irradiated quiescent HSPCs (CD45.1) immediately following IR exposure into lethally-irradiated WT (CD45.2) recipient mice and monitored them over 4 months post-transplantation for development of hematological abnormalities and genomic instability (Figure 7C). As expected, we observed a dose-dependent decrease in engraftment of IR-exposed HSPCs compared to unirradiated HSPCs, with no long-term hematopoietic reconstitution provided by 6Gy-treated HSPCs (data not shown). At 4 months post-transplantation, none of the engrafted mice developed leukemia or showed outward signs of hematological abnormalities in the peripheral blood and bone marrow (data not shown). CD45.1 donor-derived HSPCs and MPs were then isolated from pools of mice reconstituted with 2Gy-irradiated HSPCs and used, respectively, for secondary transplantation and SKY analysis. In 3 out of 4 2Gy-treated HSPC cohorts, a significant number of donor-derived MPs displayed genomic abnormalities including the presence of the same t(16;17) balanced chromosomal translocation in ~55% of cohort I2 donor-derived MPs (Figure 7E and Table S3). This result indicates the clonal expansion of a single mutated HSPC. The complete loss of engraftment that was observed following secondary transplantation of donor-derived cohort I2 HSPCs (Figure 7E), further suggest the presence of a mutation(s) associated with HSC exhaustion and bone marrow failure. Taken together, these findings indicate that misrepaired HSPCs can survive at relatively high frequencies *in vivo*, and can contribute either to the direct expansion of aberrant clones (as in cohort I2) or, more often, to the maintenance of a background of genomic alterations (as in cohorts I3 and I4), some of which could be pre-malignant.

DISCUSSION

Defects in DNA damage responses that cause accumulation of DNA damage and loss of DNA repair capacity, are broadly associated with organ failure, cancer, aging and stem cell abnormalities (Hanahan and Weinberg, 2000; Park and Gerson, 2005). The decline in tissue

NIH-PA Author Manuscript

NIH-PA Author Manuscript

NIH-PA Author Manuscript

function observed with age has also been correlated with impaired stem cell activity (Chambers and Goodell, 2007; Geiger and Rudolph, 2009). However, much remains to be elucidated about the mechanisms by which DNA damage is repaired in adult stem cells and whether mutation(s) arising from aberrant repair contribute to aging and/or susceptibility to cancer in these self-renewing populations. In this study, we investigated how blood-forming HSCs respond to DNA-damaging IR exposure, determined the extent to which they use the error-prone NHEJ repair mechanism, and assessed the consequences of such mutagenic DNA repair for their biological functions. We identify some of the key molecular mechanisms that ensure HSCs resistance to IR-mediated cell killing and provide a mechanistic explanation for why HSCs are at greater risk of accumulating mutations than other cells in the hematopoietic system. Our results demonstrate that the prevalent DNA repair mechanism active in quiescent HSCs is prone to generating mutations.

Long-lived HSCs are essential for hematopoietic homeostasis and, as we show here, have unique cell-intrinsic mechanisms ensuring their survival (Figure S7). These likely include enhanced pro-survival gene expression and robust induction of DNA damage checkpoints (*i.e*., ATM, p53) leading to a strong p53-mediated induction of both pro-apoptotic genes (*i.e*., *puma*, *noxa*, *bak*) and *p21* expression. We postulate that high basal levels of pro-survival factors likely limit IR-mediated cell killing in HSCs and instead favor *p21*-mediated growth arrest, DNA repair and survival as has already been observed in other cellular contexts (Abbas et al., 2009). This prominent role for *p21* in normal HSCs may explain why it has been found to have such an important function maintaining the DNA damage response and self-renewal properties of leukemic HSCs transformed by the *PML-RAR* oncogene (Viale et al., 2009). Interestingly, we show that normal HSCs that have been induced to proliferate either by *in vitro* culturing or *in vivo* mobilization treatment have decreased overall expression of *bcl2*-family pro-survival genes and display constitutively higher levels of apoptosis than quiescent HSCs. However, this rewiring of the apoptotic machinery does not result in loss of radioprotection nor in any significant increase in IR-mediated cell killing of proliferating HSCs, as observed in MPs, which indicates that additional, still unexplored, survival mechanism(s) also contribute to the specific protection of this self-renewing compartment. It is likely that maintenance of low levels of ROS (Tothova et al., 2007) and other fundamental mechanisms of cellular detoxification contribute to the enhanced survival of long-lived HSCs. It will also be interesting to confirm that endogenous HSCs in the bone marrow space display the same behavior following radiation insults than isolated HSCs *ex vivo*.

In terms of organ maintenance, it is logical to keep long-lived HSCs quiescent *in vivo* to guard them against DNA replication errors and damage associated with metabolic stress (Rossi et al., 2007; Orford and Scadden, 2008). Our *ex vivo* analyses demonstrate that a substantial limitation of HSC quiescence is reduced elimination of damaged HSCs by apoptosis and an increased likelihood of mutagenesis due to the use of error-prone DNA repair mechanisms (Figure S7). This conclusion is further supported by the observation that HR-competent proliferating HSCs have significantly decreased risk of acquiring mutation(s), which likely results from their use of a high fidelity repair mechanism. Our transplantation experiments directly demonstrate that damaged HSCs, which have undergone DNA repair and acquired mutation(s) during this process, can persist *in vivo* at relatively high frequencies and contribute either to the clonal expansion of aberrant cells or to the maintenance of cells with genomic alterations. Both events could predispose mutated HSCs to loss of function and/or cancer development and their occurrence is likely due to the stochastic combination of cell-intrinsic effects provided by the acquired mutation(s) and selection pressure *in vivo*. Although we have analyzed only a small number of transplanted cohorts thus far, we observed at least one case of each of the two possible mutagenic outcomes: mutation(s) providing either growth or survival advantages that are clonally

NIH-PA Author Manuscript

NIH-PA Author Manuscript

NIH-PA Author Manuscript

amplified (cohort I2) and, more frequently, non-essential “passenger” mutation(s) that appear to be maintained but not expanded *in vivo* (cohorts I3 and I4). These results are consistent with the cytogenetic pattern of human hematological malignancies, where only a handful of recurring translocations, deletions and inversions are associated with specific diseases (Look, 1997) and clonally expanded in the context of either a high or low background of genomic alterations (Radtke et al., 2009). They also extend the conclusion of a previous study performed with multipotent hematopoietic cells differentiated *in vitro* from mouse embryonic stem (ES) cells, which showed that immature hematopoietic progenitors were particularly susceptible to the formation of chromosomal rearrangements analogous to those found in human hematological malignancies (Francis and Richardson, 2007). Moreover, our findings suggest that vulnerability to mutagenesis might be a general property of all quiescent stem cell populations either normal or cancerous. They highlight why quiescent leukemic stem cells (LSCs), which currently survive therapeutic treatment in CML (Holyoake et al., 1999) and acute myeloid leukemia (AML) (Guan et al., 2003), represent a dangerous reservoir for additional mutations that is likely to contribute to disease relapse and/or evolution.

Our results provide the beginning of a molecular understanding of why HSCs are more likely than MPs to become transformed and trigger leukemia development (Bonnet and Dick, 1997). In contrast to HSCs, transformation of MPs must overcome significant self-destructive mechanisms. MPs are short-lived cells that are constantly replenished from the HSC compartment and are therefore expendable in terms of organ maintenance. Our results indicate that MPs are intrinsically poised to die and are mainly eliminated in response to DNA damage (Figure S7). When compared to HSCs, MPs have a much-attenuated p53-mediated DDR. However, despite its limited extent, p53-mediated induction of pro-apoptotic genes is not counter-balanced by high basal levels of pro-survival factors as seen in HSCs and occurs with only a weak induction of *p21*, thereby leading mostly to cell elimination. As a consequence, mutations resulting in transformation of the MP compartment are unlikely to become established unless the cells gain substantial survival advantage(s) either by inheriting mutations from the HSC compartment (as observed with *BCR/ABL1* during chronic myelogenous leukemia (CML) progression) (Jamieson et al., 2005) or by directly acquiring leukemia-associated fusion genes with major “re-programming” activity, such as *MLL* translocations (Krivtsov et al., 2006).

Our results may also explain some aspects of the loss of function occurring in HSCs with age. Age-related defects in the hematopoietic system include a decline in the adaptive immune system called immunosenescence and the development of a broad spectrum of age-related hematological disorders (*i.e*., myeloproliferative neoplasms, leukemia, lymphoma, bone marrow failure) that have been linked to changes in the biological function of aged HSCs (Chambers and Goodell, 2007; Geiger and Rudolph, 2009). Gene expression studies and analysis of genetically modified mice also indicate that errors in DNA repair and poorly maintained genomic stability are among the main driving forces for HSC aging (Rossi *et al*., 2007). Our findings suggest that accumulation of NHEJ-mediated mutation(s) over a lifetime could dramatically hinder HSC performance and be a major contributor to the loss of function observed in aged HSCs and the development of age-related hematological disorders.

Finally, our results may have direct clinical applications for minimizing the development of therapy-related cancers following cytotoxic therapy (Allan and Travis, 2005). Many solid tumors and hematological malignancies are currently treated with DNA damaging agents, which may result in therapy-related myeloid leukemia. Our work suggests that cytotoxic therapies might inadvertently mutate the patient's own quiescent HSCs by forcing them to undergo DNA repair using a mutagenic mechanism. Specifically, we show that proliferating

NIH-PA Author Manuscript

NIH-PA Author Manuscript

NIH-PA Author Manuscript

HSCs have significantly decreased mutation rates, with no observed changes in their radioresistance, suggesting that it might be beneficial to induce HSCs to cycle prior to therapy with DNA damaging agents to enhance DNA repair fidelity and reduce the risk of leukemia development. While this possibility remains to be tested, it offers exciting new directions for limiting the deleterious side effects of cancer treatment.

EXPERIMENTAL PROCEDURES

Mice

Wild type C57Bl/6-CD45.1 and C57Bl/6-CD45.2 mice were used as donors (4–8 week old) for cell isolation and as recipient (8–12 week old) for cell transplantation. *Atm*$^{-/-}$ mice (129/sv) were purchased from the Jackson Laboratory and both transgenic H2k-*bcl2* (C57Bl/6) and *Trp53*$^{-/-}$ (FVB/N) mice have been described (Domen et al., 2000; Liu et al., 2009). Cyclophosphamide/G-CSF mobilization of HSCs was performed as described (Passegué et al., 2005).

Flow cytometry

Cell staining and enrichment for cell sorting of HSPCs, CMPs, and GMPs were performed as described (Passegué et al., 2005; Santaguida et al., 2009). Each population was double-sorted to ensure maximum purity and irradiated using a ^{137}Cs source.

Cell proliferation, apoptosis and colony formation

Cells were either plated in methylcellulose and counted on day 7 using duplicate plates per condition, or grown in liquid culture and counted on days 2, 4, 6, and 8 using triplicate wells per condition and time point. Both methylcellulose and liquid cultures were supplemented with IL-3, GM-CSF, IL-11, Flt3-L, SCF, EPO and TPO as described. Flow cytometry was used to assess apoptosis levels by intracellular staining for cleaved caspase 3, and proliferation rates by CFSE dilution assay, BrdU incorporation and 7AAD/Puronin Y staining according to the manufacturer's instructions and as described (Santaguida et al., 2009).

Gene expression and protein analyses

RNA extraction, cDNA preparation and qRT-PCR analysis were performed as described (Santaguida et al., 2009). The cDNA equivalent of 200 cells was used per reaction, each measurement was performed in triplicate and values were normalized to β-actin expression. Western blot analyses were performed using the protein content of 35,000 - 70,000 purified cells (≤ 5μg total protein) per lane.

Immunofluorescence microscopy, COMET and cytogenetic assays

For immunofluorescence staining, cells were cytospun onto poly-lysine coated slides, fixed, permeabilized and stained as described (Dodson et al., 2004). For the alkaline COMET assay, cells were embedded in agarose on slides and tested as previously described (Klaude et al., 1996). For cytogenetic studies, cultured cells were treated with 0.01 μg/ml Colcemid^{TM} for 4 hours, fixed and analyzed by FISH or SKY as previously described (Le Beau et al., 2002).

Statistics

Unpaired Student *t*-test on means ± standard deviations (error bars). N indicates the numbers of independent experiments performed.

See also Supplementary Experimental Procedures and qRT-PCR Primer Table for details

NIH-PA Author Manuscript

NIH-PA Author Manuscript

NIH-PA Author Manuscript

Supplementary Material

Refer to Web version on PubMed Central for supplementary material.

Acknowledgments

We thank Drs. David Toczyski, Zhao-Qi Wang and Martin Carroll for insights and suggestions, Elizabeth Davis for the SKY analysis, Tara Rambaldo and Bill Hyun for management of the Flow Cytrometry core facility, Dr. Gordon Shore for anti-Bid antibody gift, Dr. Willian Weiss for *Trp53*$^{-/-}$ mice, Dr. Andrew Leavitt for mobilization reagents and all members of the Passegué laboratory for comments and discussion. M.M. is supported by a CIRM pre-doctoral training grant. This work was supported by a PHS P01 CA40046 to M.M.L., a Science Foundation Ireland PI award to C.G.M. and a CIRM New Investigator Award and Rita Allen Scholar Award to E.P. The authors have no financial interests to disclose.

References

Abbas T, Dutta A. p21 in cancer: intricate networks and multiple activities. Nat Rev Cancer. 2009; 9:400–414. [PubMed: 19440234]

Allan JM, Travis LB. Mechanisms of therapy-related carcinogenesis. Nat Rev Cancer. 2005; 5:943–955. [PubMed: 16294218]

Bonnet D, Dick JE. Human acute myeloid leukemia is organized as a hierarchy that originates from a primitive hematopoietic cell. Nat Med. 1997; 3:730–737. [PubMed: 9212098]

Chambers SM, Goodell MA. Hematopoietic stem cell aging: wrinkles in stem cell potential. Stem Cell Rev. 2007; 3:201–211. [PubMed: 17917133]

Dodson H, Bourke E, Jeffers LJ, Vagnarelli P, Sonoda E, Takeda S, Earnshaw WC, Merdes A, Morrison C. Centrosome amplification induced by DNA damage occurs during a prolonged G2 phase and involves ATM. EMBO J. 2004; 23:3864–3873. [PubMed: 15359281]

Domen J, Cheshier SH, Weissman IL. The role of apoptosis in the regulation of hematopoietic stem cells: Overexpression of Bcl-2 increases both their number and repopulation potential. J Exp Med. 2000; 191:253–264. [PubMed: 10637270]

Down JD, Boudewijn A, van Os R, Thames HD, Ploemacher RE. Variation in radiation sensitivity and repair among different hematopoietic stem cell subsets following fractionated irradiation. Blood. 1995; 86:122–127. [PubMed: 7795217]

Francis R, Richardson C. Multipotent hematopoietic cells susceptible to alternative double-strand break repair pathways that promote genome rearrangements. Genes Dev. 2007; 21:1064–1074. [PubMed: 17473170]

Geiger H, Rudolph KL. Aging in the lympho-hematopoietic stem cell compartment. Trends Immunol. 2009; 30:360–365. [PubMed: 19540806]

Guan Y, Gerhard B, Hogge DE. Detection, isolation, and stimulation of quiescent primitive leukemic progenitor cells from patients with acute myeloid leukemia (AML). Blood. 2003; 101:3142–3149. [PubMed: 12468427]

Hanahan D, Weinberg RA. The Hallmarks of Cancer. Cell. 2000; 100:57–70. [PubMed: 10647931]

Holyoake T, Jiang X, Eaves C, Eaves A. Isolation of highly quiescent subpopulation of primitive leukemic cells in chronic myelogenous leukemia. Blood. 1999; 94:2056–2064. [PubMed: 10477735]

Ito K, Hirao A, Arai F, Matsuoka S, Takuo K, Hamaguchi I, Nomiyama K, Hosokawa K, Sakurada K, Nakagata N, Ikeda Y, Mak TW, Suda T. Regulation of oxidative stress by ATM is required for self-renewal of haematopoietic stem cells. Nature. 2004 Oct 21; 431(7011):997–1002. [PubMed: 15496926]

Jamieson CH, Ailles LE, Dylla SJ, Muijtjens M, Jones C, Zehnder JL, Gotlib J, Li K, Manz MG, Keating A, et al. Granulocyte-macrophage progenitors in chronic myelogenous leukemia are candidate leukemia stem cells that activate the beta-catenin pathway. N Engl J Med. 2004; 351:657–667. [PubMed: 15306667]

Klaude M, Eriksson S, Nygren J, Ahnström G. The comet assay: mechanisms and technical considerations. Mutat Res. 1996; 363:89–96. [PubMed: 8676929]

NIH-PA Author Manuscript

NIH-PA Author Manuscript

NIH-PA Author Manuscript

Krivtsov AV, Twomey D, Feng Z, Stubbs MC, Wang Y, Faber J, Levine JE, Wang J, Hahn WC, Gilliland DG, et al. Transformation from committed progenitor to leukaemia stem cell initiated by MLL-AF9. Nature. 2006; 442:818–822. [PubMed: 16862118]

Le Beau MM, Bitts S, Davis EM, Kogan SC. Recurring chromosomal abnormalities in leukemia in PML-RARA transgenic mice parallel human acute promyelocytic leukemia. Blood. 2002; 99:2985–2991. [PubMed: 11929790]

Liu Y, Elf SE, Miyata Y, Sashida G, Liu Y, Huang G, Di Giandomenico S, Lee JM, Deblasio A, Menendez S, Antipin J, Reva B, Koff A, Nimer SD. p53 regulates hematopoietic stem cell quiescence. Cell Stem Cell. 2009; 4:37–48. [PubMed: 19128791]

Lombard DB, Chua KF, Mostoslavsky R, Franco S, Gostissa M, Alt FW. DNA repair, genome stability, and aging. Cell. 2005; 120:497–512. [PubMed: 15734682]

Look A. Oncogenic transcription factors in the human acute leukemias. Science. 1997; 278:1059–1064. [PubMed: 9353180]

Meijne EI, van der Winden-van Groenewegen RJ, Ploemacher RE, Vos O, David JA, Huiskamp R. The effects of x-irradiation on hematopoietic stem cell compartments in the mouse. Exp Hematol. 1991; 19:617–623. [PubMed: 1893947]

Nijnik A, Woodbine L, Marchetti C, Dawson S, Lambe T, Liu C, Rodrigues NP, Crockford TL, Cabuy E, Vindigni A, et al. DNA repair is limiting for haematopoietic stem cells during ageing. Nature. 2007; 447:686–690. [PubMed: 17554302]

Orford KW, Scadden DT. Deconstructing stem cell self-renewal: genetic insights into cell-cycle regulation. Nat Rev Genet. 2008; 9:115–128. [PubMed: 18202695]

Orkin SH, Zon LI. Hematopoiesis: an evolving paradigm for stem cell biology. Cell. 2008; 132:631–644. [PubMed: 18295580]

Park Y, Gerson SL. DNA repair defects in stem cell function and aging. Ann Rev Med. 2005; 56:495–508. [PubMed: 15660524]

Passegué E, Wagers AJ, Guiriato S, Anderson WC, Weissman IL. Global analysis of proliferation and cell cycle gene expression in the regulation of hematopoietic stem and progenitor cell fates. J Exp Med. 2005 Dec 5; 202(11):1599–1611. [PubMed: 16330818]

Radtke I, Mullighan CG, Ishii M, Su X, Cheng J, Ma J, Ganti R, Cai Z, Goorha S, Pounds SB, Cao X, Obert C, Armstrong J, Zhang J, Song G, Ribeiro RC, Rubnitz JE, Raimondi SC, Shurtleff SA, Downing JR. Genomic analysis reveals few genetic alterations in pediatric acute myeloid leukemia. Proc Natl Acad Sci USA. 2009 Aug 4; 106(31):12944–12949. Epub 2009 Jul 27. [PubMed: 19651601]

Rossi DJ, Bryder D, Seita J, Nussenzweig A, Hoeijmakers J, Weissman IL. Deficiencies in DNA damage repair limit the function of haematopoietic stem cells with age. Nature. 2007; 447:725–729. [PubMed: 17554309]

Sancar A, Lindsey-Boltz LA, Unsal-Kacmaz K, Linn S. Molecular mechanisms of mammalian DNA repair and the DNA damage checkpoints. Annu Rev Biochem. 2004; 73:39–85. [PubMed: 15189136]

Santaguida M, Schepers K, King B, Sabnis AJ, Forsberg EC, Attema JL, Braun BS, Passegué E. JunB protects against myeloid malignancies by limiting hematopoietic stem cell proliferation and differentiation without affecting self-renewal. Cancer Cell. 2009 Apr 7; 15(4):341–352. [PubMed: 19345332]

Tothova Z, Kollipara R, Huntly BJ, Lee BH, Castrillon DH, Cullen DE, McDowell EP, Lazo-Kallanian S, Williams IR, Sears C, et al. FoxOs are critical mediators of hematopoietic stem cell resistance to physiologic oxidative stress. Cell. 2007; 128:325–339. [PubMed: 17254970]

Viale A, De Franco F, Orleth A, Cambiaghi V, Giuliani V, Bossi D, Ronchini C, Ronzoni S, Muradore I, Monestiroli S, et al. Cell-cycle restriction limits DNA damage and maintains self-renewal of leukaemia stem cells. Nature. 2009; 457:51–57. [PubMed: 19122635]

Wang W. Emergence of a DNA-damage response network consisting of Fanconi anaemia and BRCA proteins. Nat Rev Genet. 2007; 8:735–748. [PubMed: 17768402]

Weinstok DM, Richardson CA, Elliott B, Jasin M. Modeling oncogenic translocations: distinct roles for double-strand break repair pathways in translocation formation in mammalian cells. DNA Repair (Amst.). 2006 Sep 8; 5(9-10):1065–1074. Epub 2006 Jul 11. [PubMed: 16815104]

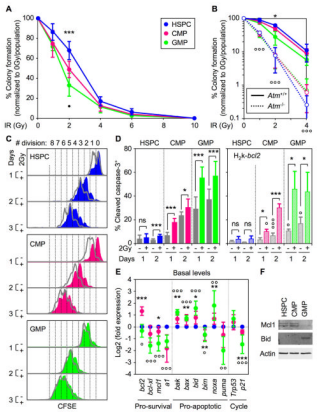

Figure 1. HSPCs are intrinsically radioresistant and survive IR-induced cell killing

(**A**) Clonogenic survival assay of irradiated cells in methylcellulose (n = 9; ***p ≤ 0.001 [CMPs and GMPs *vs*. HSPCs]; •p ≤ 0.05 [GMPs *vs*. CMPs]).

(**B**) Clonogenic survival assay of irradiated $Atm^{-/-}$ cells in methylcellulose (n = 3; *p ≤ 0.05 [$Atm^{+/+}$ GMPs *vs*. $Atm^{+/+}$ HSPCs]; °°°p ≤ 0.001 [$Atm^{-/-}$ *vs*. $Atm^{+/+}$ populations]).

(**C**) Representative example of CFSE dilution assay in unirradiated (grey) or 2Gy-irradiated (color) cells grown for up to 3 days in liquid media (n = 4).

(**D**) Intracellular cleaved caspase 3 staining in unirradiated (grey) or 2Gy-irradiated WT (left side; solid colors; n = 10) or H2k-*bcl2* (right side; striped colors; n = 3) cells grown for up to 2 days in liquid media (p ≤ 0.001, *p ≤ 0.05 [unirradiated *vs*. irradiated cells]; °°°p ≤ 0.001, °p ≤ 0.05 [H2k-*bcl2 vs.* WT cells]; ns: not significant).

(**E**) QRT-PCR analysis of the basal expression level of *bcl2*-family pro-survival and pro-apoptotic genes, *Trp53* and *p21* in freshly isolated cells. Results are expressed as log2 fold expression compared to levels measured in HSPCs (n = 6; ***p ≤ 0.001, **p ≤ 0.01, *p ≤ 0.05 [CMPs *vs*. HSPCs]; °°°p ≤ 0.001, °°p ≤ 0.01, °p ≤ 0.05 [GMPs *vs*. HSPCs]).

(**F**) Western blot analysis of Mcl-1 and Bid protein levels in purified cells (protein extracted from 35,000 isolated cells per lane; β-actin is used as loading control).

See also Figure S1.

NIH-PA Author Manuscript NIH-PA Author Manuscript NIH-PA Author Manuscript

NIH-PA Author Manuscript

NIH-PA Author Manuscript

NIH-PA Author Manuscript

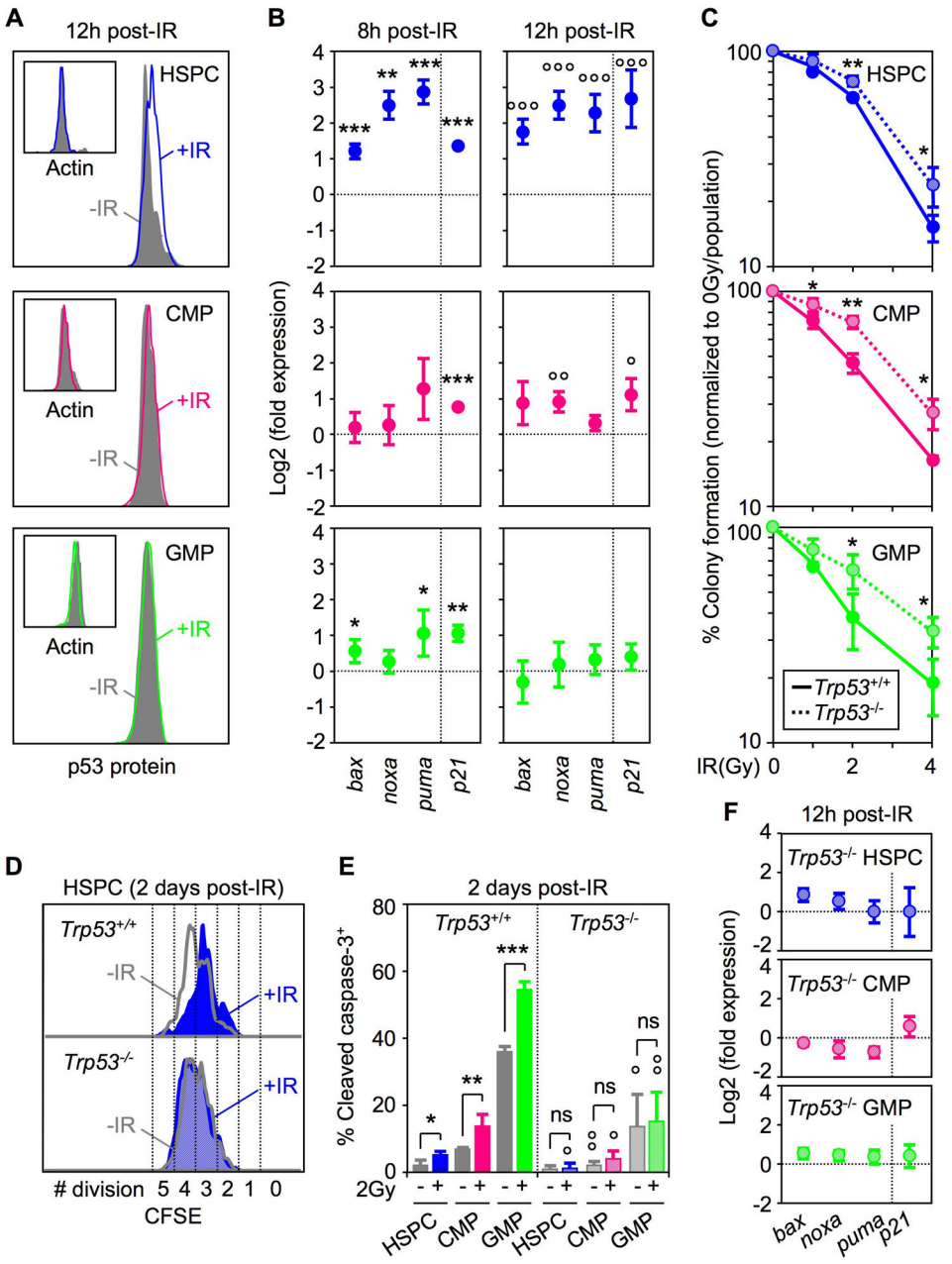

Figure 2. Dual role for p53-mediated DNA damage response in HSPCs and myeloid progenitors

(**A**) Intracellular FACS analysis of p53 and actin protein levels in unirradiated (-IR) or 2Gy irradiated (+IR) mice 12 hours after exposure.

(**B**) QRT-PCR analysis of p53 target genes in WT cells 8 and 12 hours after 2Gy IR treatment. Results are expressed as log2 fold expression compared to levels measured in unirradiated cells cultured in the same conditions (n = 3; ***p ≤ 0.001, **p ≤ 0.01, *p ≤ 0.05) or 12 hours (n = 3; °°°p ≤ 0.001, °°p ≤ 0.01, °p ≤ 0.05).

(**C**) Clonogenic survival assay of irradiated *Trp53*$^{-/-}$ cells in methylcellulose (n = 3; **p ≤ 0.01, *p ≤ 0.05 [*Trp53*$^{-/-}$ *vs. Trp53*$^{+/+}$ cells]).

(**D**) Example of CFSE dilution assay in unirradiated (-IR: grey) or 2Gy-irradiated (+IR: blue) *Trp53*$^{+/+}$ (solid) and *Trp53*$^{-/-}$ (striped) HSPCs grown for 2 days in liquid media (n = 3).

NIH-PA Author Manuscript

NIH-PA Author Manuscript

NIH-PA Author Manuscript

(**E**) Intracellular cleaved caspase 3 staining in unirradiated (grey) or 2Gy-irradiated $Trp53^{+/+}$ (solid colors) and $Trp53^{-/-}$ (striped colors) cells grown for up to 2 days in liquid media (n = 3; ***p ≤ 0.001, ** p ≤ 0.01, *p ≤ 0.05 [unirradiated *vs*. irradiated cells]; °°p ≤ 0.01, °p ≤ 0.05 [$Trp53^{-/-}$ *vs.* $Trp53^{+/+}$ cells]; ns: not significant).
(**F**) QRT-PCR analysis of p53-target genes in $Trp53^{-/-}$ cells 12 hours after 2Gy IR treatment. Results are expressed as log2 fold expression compared to levels measured in unirradiated $Trp53^{-/-}$ cells cultured in the same conditions (n = 3).
See also Figure S2

NIH-PA Author Manuscript

NIH-PA Author Manuscript

NIH-PA Author Manuscript

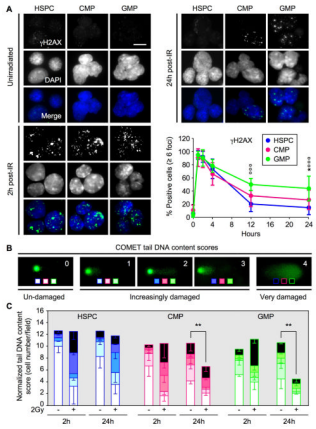

Figure 3. Ongoing DNA repair in HSPCs versus cell elimination in myeloid progenitors

(**A**) Immunofluorescence microscopy of ionizing radiation-induced foci (IRIF) of γH2AX in unirradiated or 2Gy-irradiated HSPCs (n = 13), CMPs (n = 8) and GMPs (n = 10). The percentage of positive cells (≥6 γH2AX positive foci) is shown over 24 hours (*$p \leq 0.05$ [CMPs *vs*. HSPCs]; °°°$p \leq 0.001$ [GMPs *vs*. HSPCs]; scale bar = 10 μm).

(**B**) Representative examples of COMET tail DNA content scoring from un-damaged (0), increasingly damaged (1–3) to very damaged (4) cells.

(**C**) Quantification of tail DNA content scores in unirradiated or 2Gy irradiated HSPCs, CMPs and GMPs after 2 and 24 hours. Results are normalized to the number of cells counted per field (n = 3; **$p \leq 0.01$).

See also Table S1.

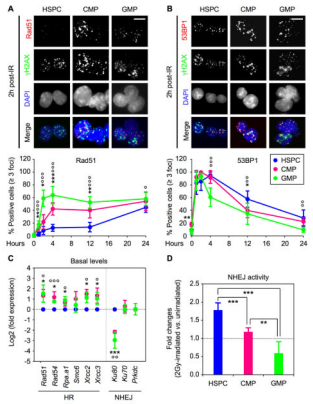

Figure 4. High NHEJ-mediated DNA repair mechanism in HSPCs

(**A**) Immunofluorescence microscopy of Rad51 IRIF in unirradiated and 2Gy-irradiated HSPCs (n = 5), CMPs (n = 6) and GMPs (n = 8). The percentage of positive cells (≥3 Rad51 positive foci) is shown over 24 hours (***p ≤ 0.001, **p ≤ 0.01, *p ≤ 0.05 [CMPs *vs*. HSPCs]; °°°p ≤ 0.001, °p ≤ 0.05 [GMPs *vs*. HSPCs]; scale bar = 10 μm).

(**B**) Immunofluorescence microscopy of 53BP1 IRIF in unirradiated and 2Gy-irradiated HSPCs (n = 9), CMPs (n = 7) and GMPs (n = 9). The percentage of positive cells (≥3 53BP1 positive foci) is shown over 24 hours (***p ≤ 0.001, *p ≤ 0.05 [CMPs *vs*. HSPCs]; °°°p ≤ 0.001, °°p ≤ 0.01 [GMPs *vs*. HSPCs]; scale bar = 10 μm).

(**C**) QRT-PCR analysis of homologous recombination (HR) and nonhomologous end joining (NHEJ) DNA repair genes in freshly isolated cells. Results are expressed as log2 fold expression compared to levels measured in HSPCs (n = 3; ***p ≤ 0.001, *p ≤ 0.05 [CMPs *vs*. HSPCs]; °°°p ≤ 0.001, °°p ≤ 0.01, °p ≤ 0.05 [GMPs *vs*. HSPCs]).

(**D**) Quantification of NHEJ activity in unirradiated and 2Gy-irradiated cells. Results are expressed as fold changes upon IR-treatment (n = 5; ***p ≤ 0.001, **p ≤ 0.01).

See also Figure S3 and Figure S4.

NIH-PA Author Manuscript NIH-PA Author Manuscript NIH-PA Author Manuscript

NIH-PA Author Manuscript
NIH-PA Author Manuscript
NIH-PA Author Manuscript

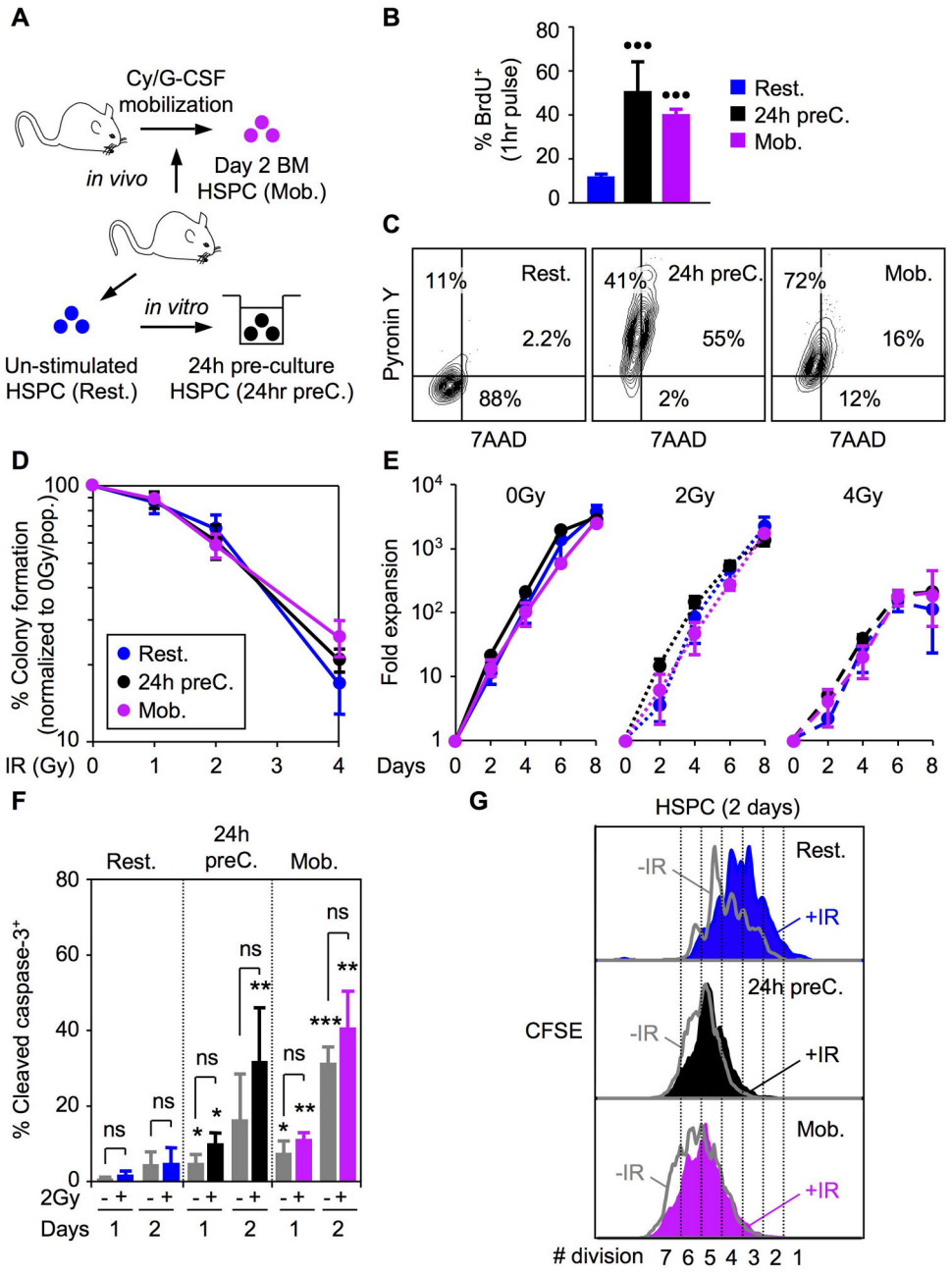

Figure 5. Similar radioresistance in quiescent and proliferating HSPCs

(A) *In vitro* 24 hour pre-culture (24hr preC) and *in vivo* cyclosphosphamide/G-CSF mobilization (Mob.) strategies used to induce proliferation of quiescent (Rest.) HSPCs.

(**B**) Proliferation rates measured after 1 hour BrdU pulse *in vitro* (n = 3; •••p ≤ 0.001; [proliferating HSPCs *vs*. resting HSPCs]).

(**C**) Quiescence status measured by intracellular 7AAD/Pyronin Y staining.

(**D**) Clonogenic survival assay in methylcellulose (n = 3).

(**E**) Growth in liquid media (n = 3).

(**G**) Intracellular cleaved caspase 3 staining in unirradiated (grey) or 2Gy-irradiated (color) resting and proliferating HSPCs grown for up to 2 days in liquid media (n = 3; ***p ≤

NIH-PA Author Manuscript

NIH-PA Author Manuscript

NIH-PA Author Manuscript

0.001, **p ≤ 0.01, *p ≤ 0.05 [proliferating HSPCs ± IR *vs*. resting HSPCs ± IR]; ns: not significant).
(**F**) Example of CFSE dilution assay in unirradiated (grey) or 2Gy-irradiated (color) quiescent and proliferating HSPCs grown for 2 days in liquid media (n = 3).
See also Figure S5.

NIH-PA Author Manuscript

NIH-PA Author Manuscript

NIH-PA Author Manuscript

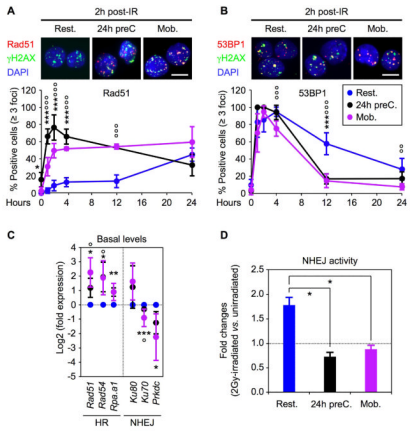

Figure 6. Proliferating HSPCs shift to HR-mediated DNA repair mechanism

(**A**) Immunofluorescence microscopy of Rad51 IRIF in 2Gy-irradiated resting HSPCs (n = 5), 24h pre-cultured HSPCs (n = 3) and mobilized HSPCs (n = 5). The percentage of positive cells (≥ 3 Rad51 positive foci) is shown over 24 hours (***p ≤ 0.001, *p ≤ 0.05 [24h preC. *vs*. Rest. HSPCs]; °°°p ≤ 0.001 [Mob. *vs*. Rest. HSPCs]; scale bar = 10 μm).

(**B**) Immunofluorescence microscopy of 53BP1 IRIF in 2Gy-irradiated resting HSPCs (n = 9), 24h pre-cultured HSPCs (n = 3) and mobilized HSPCs (n = 5). The percentage of positive cells (≥ 3 53BP1 positive foci) is shown over 24 hours (***p ≤ 0.001 [24hr preC. *vs*. Rest. HSPCs]; °°°p ≤ 0.001, °°p ≤ 0.01 [Mob. *vs*. Rest. HSPCs]; scale bar = 10 μm).

(**C**) QRT-PCR analysis of HR and NHEJ repair genes in resting and proliferating HSPCs (n = 3; ***p ≤ 0.001, **p ≤ 0.01, *p ≤ 0.05 [24h preC *vs*. Rest. HSPCs]; °°°p ≤ 0.001, °°p ≤ 0.01, °p ≤ 0.05 [Mob. *vs*. Rest. HSPCs]).

(**D**) Quantification of NHEJ activity in unirradiated and 2Gy-irradiated resting and proliferating HSPCs. Results are average ± SEM (error bars) of 2 (24h preC. and Mob. HSPCs) to 5 (Rest. HSPCs) independent experiments and are expressed as fold changes upon IR-treatment (*p 0.05).

See also Figure S4 and Figure S5.

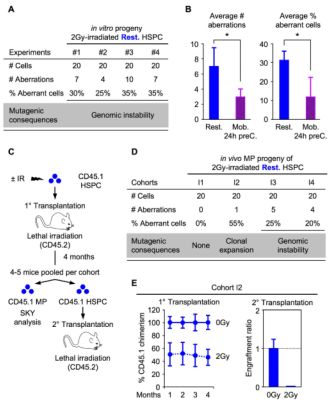

Figure 7. Mutagenic DNA repair in quiescent HSPCs

(**A**) Summary of the SKY analyses performed on the *in vitro* progeny of 2Gy-irradiated quiescent HSPCs.

(**B**) Average number of genomic rearrangement (left side) and percentage (%) of aberrant cells (right side) identified by SKY analysis in the *in vitro* progeny of 2Gy-irradiated quiescent (Rest.; n = 4) and proliferating (Mob./24h preC; n = 3) HSPCs (*$p \leq 0.05$).

(**C**) Experimental design of the *in vivo* analysis of 2Gy-irradiated HSPCs assessing long-term reconstitution and genomic instability.

(**D**) Summary of the SKY analysis performed on the *in vivo* MP progeny of 2Gy-irradiated quiescent HSPCs 4 months after transplantation.

(**E**) In cohort I2, 1,500 ±IR HSPC together with 300,000 Sca-1-depleted helper bone marrow cells were transplanted per recipient (n = 5 [0Gy] and 4 [2Gy] mice per group). Long-term reconstitution was measured by sustained CD45.1 chimerism in the peripheral blood of primary transplanted mice (left graph; expressed as percent of the engraftment provided by unirradiated HSPCs) and secondary transplantation of donor-derived HSPCs re-isolated from pooled primary transplanted animals (right graph; expressed as engraftment ratio of $CD45.1^+$ cells at 4 months post-transplantation; n = 4 [0Gy] and 5 [2Gy] mice per group).

See also Figure S6, Table S2 and Table S3.

NIH-PA Author Manuscript NIH-PA Author Manuscript NIH-PA Author Manuscript